Electron Transfer Dynamics in Quantum Dot/Titanium Dioxide Composites Formed by in Situ Chemical Bath Deposition

Jeff L. Blackburn,*,†,‡ Don C. Selmarten,† and Arthur J. Nozik†,‡

Center for Basic Science, National Renewable Energy Laboratory, Golden, Colorado 80401, and Department of Chemistry and Biochemistry, University of Colorado, Boulder, Colorado 80309

Received: September 8, 2003; In Final Form: November 6, 2003

We present experimental transient absorption (TA) results on the dynamics of electron relaxation and electron transfer in cadmium sulfide quantum dots (QDs) grown by chemical bath deposition techniques on nanocrystalline oxide substrates. The quantum dots are prepared in situ in nanocrystalline titanium dioxide (TiO_2) and zirconium oxide (ZrO_2) films. The conduction band offset between the CdS QDs and TiO_2 allows for efficient electron injection from the photoexcited QDs into the conduction band of TiO_2. An unprecedented peak is seen in the transient absorption spectrum, which may be used to track the spectral response of the QD/TiO_2 composites. Dynamic measurements in the visible and mid-IR are used to evaluate the time scale of the electron injection process. The TA dynamics for these systems are found to be multiexponential. A comparison of the TA dynamics for CdS/TiO_2 and CdS/ZrO_2 composites in the visible and mid-IR region indicates that electron transfer occurs on the time scale of ∼10−50 ps.

Introduction

Photosensitization of nanocrystalline titanium dioxide by semiconductor nanocrystals, or quantum dots (QDs), has received much attention.[1−11] The energetic offset between the QD and TiO_2 conduction bands promotes charge separation, making such composites attractive for solar energy conversion and photocatalysis. One simple method to make such electrodes is the in situ preparation of QDs within high surface area nanocrystalline TiO_2 films using the "successive ionic layer adsorption and reaction" (SILAR) technique.[1,3,9] This technique has been successful in the preparation of a variety of II−VI QD−TiO_2 composites with photocurrent quantum yields up to ∼70%.[3]

The research on QD sensitization of high surface area TiO_2 electrodes builds on a wealth of research involving organic dyes as sensitizers.[12−14] To date, the time scale of electron transfer, forward or reverse, from QDs into TiO_2 is poorly understood, though some reports are available.[9−11] Transient absorption (TA) spectroscopy is a powerful tool capable of investigating ultrafast charge transfer across such interfaces, but extensive TA studies of in situ grown QD−TiO_2 composites have not been reported.

In this report, we examine the dynamics of electron injection from SILAR CdS QDs into TiO_2. A peak is observed in the TA spectra of the composites that may be used to closely follow the growth of quantized CdS particles in the TiO_2 films. An analysis of the TA dynamics in the visible and mid-IR regions is used to evaluate the time scale for electron injection, which is found to occur in ∼10−50 ps.

Experimental Section

TiO_2 and ZrO_2 nanocrystalline films were prepared by a method similar to that reported by Zaban and co-workers.[15] The synthesis for the TiO_2 and ZrO_2 colloids is based on the controlled hydrolysis of the appropriate precursor, titanium(IV) isopropoxide or zirconium(IV) propoxide, and subsequent autoclaving at 230 and 220 °C, respectively. The resulting sol−gels are mixed with Carbowax (∼40 wt %), spread onto sapphire substrates, and sintered at 450 °C for 1 h.

The CdS−TiO_2 and CdS−ZrO_2 composites are prepared by the method of Weller et al.[1,3] Briefly, the sintered oxide film is dipped for 2 min into a saturated cadmium acetate solution, rinsed with deionized water, then dipped for 2 min into a 0.1 M Na_2S solution, and rinsed again. This procedure is repeated as many times as desired with each successive two-step cycle producing slightly larger CdS nanocrystals within the film.

Steady-state absorption measurements were made using a Cary 500 double beam spectrometer at a spectral resolution of 1 nm. The samples were sapphire substrates coated with the sintered TiO_2 or ZrO_2 films and then coated with CdS QDs as discussed above. To reduce the contribution of scattering, a blank TiO_2 or ZrO_2 film was used for baseline subtraction.

Steady-state photoluminescence (PL) measurements were made using a Spex 1680 Fluorolog 0.22 m double spectrometer in front face mode. The angle of the sample relative to the excitation beam was between 0° and 10°. The spectrometer uses a Xe arc lamp as the excitation source with the wavelength of excitation selected by the monochromator. The wavelength of excitation used in these experiments was 440 nm.

The transient absorption (TA) setup, based on a Clark-MXR CPA-2001 regeneratively amplified Ti:sapphire laser operating at 989 Hz and 775 nm, has been described previously.[16] For transient absorption measurements, the CdS films were cast onto sapphire windows and assembled in an airtight cell in an inert atmosphere of helium.[17] The pump fluence for all TA measurements was kept below 15 uJ cm^{-2}.

Results and Discussion

Linear Absorption Spectroscopy. The linear absorption spectra of the CdS-sensitized oxide films agree with the previous

† National Renewable Energy Laboratory.
‡ University of Colorado.

10.1021/jp0366771 CCC: $25.00
Published on Web 12/02/2003

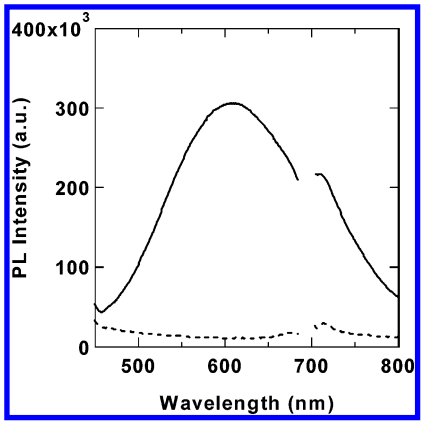

Figure 1. Steady-state photoluminescence from CdS−ZrO_2 (solid line) and CdS−TiO_2 (dashed line) composites. The excitation wavelength is 440 nm. The discontinuity at 700 nm, resulting from PL from the sapphire substrate, is removed.

findings of various groups.[1,3,9] The spectra are fairly featureless with one shoulder, presumably representing the first quantized excitonic state for the in situ prepared CdS quantum dots. This shoulder shifts red with each successive deposition cycle, indicating a reduction of quantum confinement resulting from the increase in size of the CdS quantum dots.

Photoluminescence. The steady-state photoluminescence (PL) of five-cycle CdS−TiO_2 and CdS−ZrO_2 composites is shown in Figure 1. ZrO_2 is chosen as a control because the conduction band of ZrO_2 lies too far negative to allow electron injection from the photoexcited CdS QDs. Thus, the PL originating from the photoexcited CdS−ZrO_2 composite represents the intrinsic PL from the CdS QDs. The steady-state PL of the CdS QDs on ZrO_2 is very broad and strongly red-shifted from the absorption maximum, indicative of a high degree of surface state recombination. Since the conduction band of TiO_2 lies positive of the CdS conduction band, electron injection is expected from the photoexcited CdS QDs into the TiO_2 conduction band. As shown in Figure 1, the PL is entirely quenched on the TiO_2 film, indicating efficient charge injection from the photoexcited CdS QDs into the conduction band of the TiO_2, as seen by others.[9]

Transient Absorption Spectra. Photoexcitation of semiconductor QDs generates excitons, which relax through a manifold of discrete quantized excited states before recombining. Occupation of a quantized excited state reduces the oscillator strength associated with the transition to that state, a process known as state-filling. The energetic position of the photoinduced absorption bleach resulting from state-filling is an indication of the energy of the lowest quantized excited state, and hence the size, of the CdS QDs probed in the TA experiment.

To follow the energetics of the photoinduced TA bleaching, a pump wavelength of 420 nm was chosen to selectively photoexcite only the CdS QDs. Figure 2 shows chirp-corrected transient absorption spectra taken at 2.0 ps following photoexcitation at 420 nm of a CdS−TiO_2 composite. Following photoexcitation of charge carriers within the CdS QDs, a strong positive signal results in the visible portion of the spectrum. As the number of cycles increases beyond two, it becomes evident that the photoinduced signal is a peak, which increases in magnitude and shifts to the red with each successive deposition cycle. To our knowledge, this is the first observation of size-dependent transient absorption spectra for SILAR-prepared CdS quantum dots.

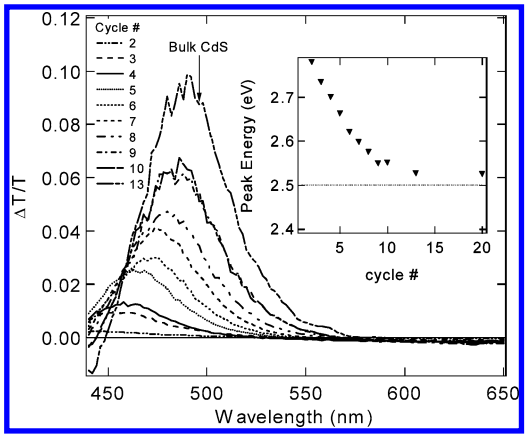

Figure 2. Transient absorption spectrum as a function of deposition cycle for a CdS−TiO_2 composite. The arrow indicates the position of the bulk band gap for CdS, 496 nm or 2.5 eV. The inset shows the energy at the peak of the TA bleach as a function of deposition cycle.

The positive photoinduced signal indicates absorption bleaching resulting from state-filling. The increase in the magnitude of the bleach results from increased light absorption due to the larger amount of CdS incorporated into the film with each cycle. The shift of the absorption bleach to the red with each successive cycle is a result of relaxing quantum confinement and a clear indication that the CdS QDs created within the film are growing in size with each successive deposition cycle. The inset shows that in early cycles small CdS QDs are produced with band gap energies more than 300 meV greater than the bulk band gap, 2.5 eV. After many cycles, the growth appears to saturate near the energy of the bulk band gap.

Transient Absorption Dynamics. Information on charge carrier dynamics may be obtained by varying the pump−probe delay at a fixed wavelength. It has been demonstrated that choosing the correct spectral probe range is useful for selectively probing electron or hole dynamics.[18−20] These reports indicate that electron dynamics in QDs are selectively probed in the visible and mid-IR range, while hole dynamics are best followed in the near-IR. We have performed TA dynamic measurements in the visible and mid-IR spectral ranges to analyze the electron transfer from photoexcited CdS QDs into TiO_2.

For these experiments, five cycles of CdS deposition were performed on TiO_2 and ZrO_2 films. For the dynamics measurements, the CdS QDs were excited at 460 nm, and probing in the visible was done directly adjacent to the pump, at 470 nm. This ensures that electrons are resonantly excited into the lowest conduction level, allowing us to ignore intraband relaxation.

Figure 3 shows the decay of the bleach at 470 nm for the TiO_2 and ZrO_2 films photoexcited at 460 nm. The bleach in the visible is sensitive only to the presence of the electron in the lowest conduction level of the CdS QD. Thus, the decay of the visible bleach represents the depopulation of the CdS excited state via recombination or trapping in the case of CdS−ZrO_2 and via recombination, trapping, and electron transfer in the case of CdS−TiO_2. If the system is assumed to be ideal and simple exponential kinetics are applied to model the depopulation of the CdS excited state, the rate equations for depopulation are as follows:

$$\text{CdS}-\text{ZrO}_2 \qquad [N]_t = [N]_0\, e^{-k_r t} \tag{1}$$

$$\text{CdS}-\text{TiO}_2 \qquad [N]_t = [N]_0\, e^{-(k_r+k_{et})t} \tag{2}$$

where k_r is the intrinsic CdS decay rate constant (trapping +

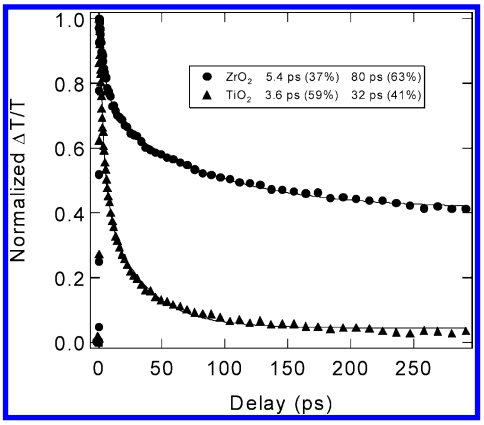

Figure 3. Visible transient absorption dynamics for CdS−TiO_2 (▲) and CdS−ZrO_2 (●) composites, five cycles each. The samples are excited at a wavelength of 460 nm and probed at 470 nm. Inset shows the results of a biexponential fit for each trace (solid lines).

recombination), k_{et} is the electron-transfer rate constant, $[N]_0$ is the initial photoexcited electron population in the lowest CdS conduction level, and $[N]_t$ is the population in the lowest CdS conduction level at time *t*. Once the intrinsic decay rate constant of the CdS electron is known by measuring the dynamics of the CdS−ZrO_2 sample, the rate constant for electron transfer to TiO_2 may be calculated by subtracting the intrinsic rate constant from the rate constant obtained from the CdS−TiO_2 dynamics.

This simple analysis is complicated by the multiexponential behavior of the decay of the visible bleach. Adsorption to TiO_2 greatly increases the rate of decay (Figure 3, inset) of the TA bleach by opening up another source of depopulation for the excited electron. Each of the two lifetime components is affected, both in magnitude and in the contribution to the overall decay. For the QDs adsorbed to TiO_2, the bleach is almost entirely decayed by ∼300 ps. The values obtained from the biexponential fit, however, may be used to calculate an estimate for the electron-transfer rate based on eqs 1 and 2. The simplest analysis treats each time constant as being independent and assumes that they each apply to separate noninteracting decay channels. Now, if it is assumed that no electron injection occurs between CdS and ZrO_2, then each rate constant obtained from the fit of the CdS−ZrO_2 decay may be treated as an independent k_r, while each rate constant obtained from the fit of the CdS−TiO_2 may be treated as a separate and independent sum of k_r and k_{et}. By comparing k_r values of 0.0125 and 0.185 ps^{-1} to [k_r + k_{et}] values of 0.0312 and 0.280 ps^{-1}, we obtained electron-transfer rates of 0.0187 and 0.095 ps^{-1}. These correspond to electron injection times of ∼50 and ∼10 ps, respectively.

It is also possible to estimate the time scale of electron transfer by calculating average lifetimes from the visible bleaching dynamics. The average lifetime may be calculated by the following expression:

$$\bar{\tau} = \frac{\sum_{i=1}^{n} \alpha_i \tau_i^2}{\sum_{i=1}^{n} \alpha_i \tau_i} \qquad (3)$$

where τ_i represents each lifetime obtained from the fit and α_i represents each corresponding preexponential factor.[21] Using the values calculated for the CdS−TiO_2 and CdS−ZrO_2 composites (inset, Figure 3), we calculated average lifetimes of 28 and 77 ps, respectively. Using eqs 2 and 3, as described above, we calculated an average electron-transfer time of 44 ps.

To further analyze the electron transfer between the CdS QDs and TiO_2, TA experiments were performed in the mid-IR range. In semiconductors, free carriers show pronounced absorption in the infrared.[22] The absorption of conduction band electrons in TiO_2 has been used to quantify electron injection rates from dyes.[13,14,23,24] In these experiments, the electron injection rate was measured as the ultrafast rise time of the mid-IR signal following photoexcitation of the adsorbed dye. Utilizing this technique for a system in which the donor (CdS) and acceptor (TiO_2) are both semiconductors with strong mid-IR absorptions presents a challenge.

It is useful to compare the dynamics of the photoinduced bleach in the visible region to the dynamics of the photoinduced absorbance in the mid-IR. As stated above, the bleach in the visible is sensitive only to the presence of the electron in the lowest conduction level of the CdS QD. Now we focus on the photoinduced absorbance in the mid-IR. It is first essential to understand that a mid-IR absorbance signal will be measured if an electron is present in the conduction band of any of the three semiconductors: CdS, TiO_2, or ZrO_2. In the CdS−ZrO_2 composite, no electron is injected into the ZrO_2 conduction band. This implies that the only species available to absorb in the mid-IR for CdS−ZrO_2 is the CdS electron, and eq 2 may be used to account for the mid-IR absorbance decay and visible bleach decay. For CdS−TiO_2 composites, however, electron injection into TiO_2 means that a mid-IR signal will be detected both from electrons in the CdS QD and from electrons in TiO_2. Assuming the same simple kinetics as utilized for eqs 1 and 2, the rate law for electron arrival in the TiO_2 is derived as

$$\text{CdS-TiO}_2 \qquad [T]_t = [N]_0\left[\frac{k_{et}}{k_{et}+k_r}(1 - e^{-(k_r+k_{et})t})\right] \qquad (4)$$

where $[T]_t$ is the electron population in the TiO_2 conduction band at time *t* and the other variables are the same as those in eqs 2 and 3. Thus, for CdS−TiO_2, the signal measured in the mid-IR will be comprised of the decay of the CdS electron (eq 2), and a rise time associated with electron arrival in the TiO_2 (eq 4).

The analysis is again complicated by the multiexponential behavior of the CdS electron relaxation. However, since electrons are excited directly into the lowest conduction level, the rise of the bleach signal and mid-IR absorbance will be coincidental and instantaneous. This means that when comparing the dynamics of the photoinduced visible bleach to the dynamics of the photoinduced IR absorbance, any electron-transfer event should manifest itself not in the rise times of these signals but in their decays. This allows us to normalize the traces to their peak magnitudes, as shown in Figure 4.

Figure 4a shows the normalized visible- and IR-probed dynamics for five cycle CdS−TiO_2 and CdS−ZrO_2 (inset) samples. First, the qualitative arguments discussed above may be seen by comparing the CdS−ZrO_2 dynamics to the CdS−TiO_2 dynamics. Because the only species measured in the CdS−ZrO_2 composite is the photoexcited CdS electron, both visible and IR dynamics are the same for this sample. This is a clear sign that in the absence of electron transfer, the visible bleaching dynamics match the induced absorbance dynamics in the mid-IR. For the case of CdS−TiO_2, the mid-IR dynamics significantly deviate from the visible dynamics. After 300 ps following photoexcitation, the visible signal has decayed to nearly zero,

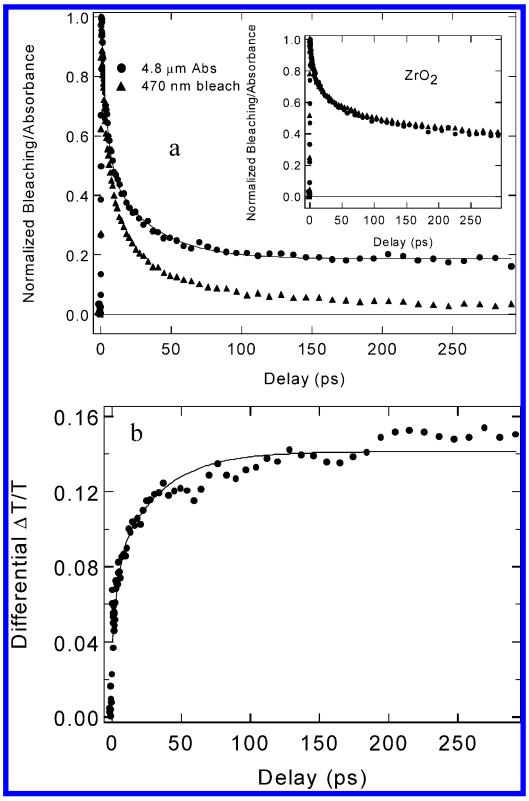

Figure 4. Comparison of the dynamics (a) of the visible bleach and mid-IR absorbance following excitation at 460 nm for a five cycle $CdS-TiO_2$ composite. The inset shows the same comparison for a five cycle $CdS-ZrO_2$ composite. Solid line shows a biexponential fit to the $CdS-TiO_2$ mid-IR dynamics with decay times of 3.7 ps (60%) and 32 ps (40%) with a positive offset of ~19%. Panel b shows the difference trace obtained by subtracting normalized bleaching dynamics from dynamics of mid-IR absorbance for the $CdS-TiO_2$ composite shown in Figure 4a. Solid line is a biexponential fit using time constants of 3.6 and 32 ps, as obtained from the kinetic analysis discussed in the text.

while approximately 20% of the mid-IR signal still remains. A biexponential fit to the $CdS-TiO_2$ mid-IR dynamics yields the same decay times and relative contributions as the fit to the bleaching dynamics. This is because both the CdS electron decay (eq 2) and the arrival of electrons in the conduction band of the TiO_2 (eq 4) are dominated by the same rate constants ($k_r + k_{et}$), only with different signs. The mid-IR fit differs only by the addition of a positive offset of ~19%, which is due to the absorbance of electrons in the TiO_2.

Finally, the electron-transfer dynamics for the $CdS-TiO_2$ conjugate can be estimated from Figure 4a by subtracting the visible bleach dynamics from the mid-IR absorbance dynamics. The result is a rising signal representing the dynamics of electron arrival into the TiO_2 conduction band (Figure 4b). As discussed above, electron arrival is dominated by the overall rate constant [$k_r + k_{et}$], which we obtained from the fits of Figures 3 and 4a. A biexponential fit of this rise time, using time constants of 3.6 and 32 ps (solid line), fits the data well, showing consistency with the other methods of analysis described above.

Summary

The peak in the TA spectra shown in these experiments allows for a more accurate measurement of the spectral response of such systems than is available from steady-state absorption. The TA dynamics of these systems are multiexponential with electron-transfer times in the range of 10−50 ps.

A useful application of the TA results is the estimate of the time scale of electron injection. Electron injection on the scale of ~10 ps must be considered in the context of the intrinsic deactivation pathways for electrons in the semiconductor QD. TA and time-resolved PL measurements (not shown) indicate several deactivation pathways exist for photoexcited electrons in the CdS QDs with time scales ranging from several picoseconds to tens of nanoseconds. Therefore, electron transfer on the time scale of tens of picoseconds should result in significantly high efficiencies for charge separation in QD-sensitized solar cells. Indeed, groups have measured up to nearly 80% photocurrent quantum yields in such cells.[1,3]

While the electron injection time for $CdS-TiO_2$ composites made by the SILAR technique has not been reported, estimates of <20[11] and 2 ps[10] have been reported for the two semiconductors coupled in a colloidal mixture.

Acknowledgment. J.L.B and A.J.N were supported by the U.S. Department of Energy, Office of Basic Energy Sciences, Division of Chemical Sciences, Geosciences, and Biosciences. D.S. was supported by the Xcel Energy Renewable Development Fund.

References and Notes

(1) Vogel, R.; Klaus, P.; Weller, H. *Chem. Phys. Lett.* **1990**, *174*, 241.

(2) Zaban, A.; Micic, O. I.; Gregg, B. A.; Nozik, A. J. *Langmuir* **1998**, *14*, 3153.

(3) Vogel, R.; Weller, H. *J. Phys. Chem.* **1994**, *98*, 3183.

(4) Kietzmann, R.; Willig, F.; Weller, H.; Vogel, R.; Nath, D. N.; Eichberger, R.; Liska, P.; Lehnert, J. *Mol. Cryst. Liq. Cryst.* **1991**, *194*, 169.

(5) Lawless, D.; Kapoor, S.; Meisel, D. *J. Phys. Chem.* **1995**, *99*, 10329.

(6) Kumar, A.; Jain, A. K. *J. Mol. Catal. A* **2001**, *165*, 265.

(7) Peter, L. M.; Jason Riley, D.; Tull, E. J.; Upul Wijayantha, K. G. *Chem. Commun.* **2002**, 1030.

(8) Sant, P. A.; Kamat, P. V. *Phys. Chem. Chem. Phys.* **2002**, *4*, 198.

(9) Plass, R.; Pelet, S.; Krueger, J.; Gratzel, M.; Bach, U. *J. Phys. Chem. B* **2002**, *106*, 7578.

(10) Evans, J. E.; Springer, K. W.; Zhang, J. Z. *J. Chem. Phys.* **1994**, *101*, 6222.

(11) Gopidas, K. R.; Bohorquez, M.; Kamat, P. V. *J. Phys. Chem.* **1990**, *94*, 6435.

(12) Hagfeldt, A.; Grätzel, M. *Acc. Chem. Res.* **2000**, *33*, 269.

(13) Asbury, J. B.; Hao, E.; Wang, Y.; Ghosh, H. N.; Lian, T. *J. Phys. Chem. B* **2001**, *105*, 4545.

(14) Asbury, J. B.; Anderson, N. A.; Hao, E.; Ai, X.; Lian, T. *J. Phys. Chem. B* **2003**, *107*, 7376.

(15) Zaban, A.; Ferrere, S.; Sprague, J.; Gregg, B. A. *J. Phys. Chem. B* **1997**, *101*, 55.

(16) Blackburn, J. L.; Ellingson, R. J.; Micic, O. I.; Nozik, A. J. *J. Phys. Chem. B* **2003**, *107*, 102.

(17) It was found that continuous photoexcitation of the sample in air induces degradation, as evidenced by a blue shift of the TA bleaching and a decrease in the magnitude of the bleach. When the cell is assembled in an inert atmosphere of helium and then examined by TA spectroscopy, the TA bleaching position and magnitude remain stable even after hours of continuous photoexcitation.

(18) Klimov, V. I.; McBranch, D. W.; Leatherdale, C. A.; Bawendi, M. G. *Phys. Rev. B* **1999**, *60*, 13740.

(19) Guyot-Sionnest, P. J.; Hines, M. A. *Appl. Phys. Lett.* **1998**, *72*, 686.

(20) Burda, C.; Link, S.; Mohamed, M.; El-Sayed, M. *J. Phys. Chem. B* **2001**, *105*, 12286.

(21) James, D. R.; Liu, Y. S.; de Mayo, P.; Ware, W. R. *Chem. Phys. Lett.* **1985**, *120*, 460.

(22) Pankove, J. I. *Optical Processes in Semiconductors*; Dover Publications, Inc.: New York, 1975.

(23) Ellingson, R. J.; Asbury, J. B.; Ferrere, S.; Ghosh, H. N.; Sprague, J.; Lian, T.; Nozik, A. J. *J. Phys. Chem. B* **1998**, *102*, 6455.

(24) Asbury, J. B.; Ellingson, R. J.; Ghosh, H. N.; Ferrere, S.; Nozik, A. J.; Lian, T. *J. Phys. Chem. B* **1999**, *103*, 3110.